Linking Taiwan's subcritical Hsuehshan Range topography and foreland basin architecture

T. Wilcox,[1] K. Mueller,[1] P. Upton,[2] Y. G. Chen,[3] S. T. Huang,[4] B. J. Yanites,[5] and G. Tucker[1]

Received 3 November 2010; revised 6 April 2011; accepted 11 May 2011; published 20 August 2011.

[1] The contemporary presence of the Puli Topographic Embayment within the Taiwanese thrust belt provides insight into processes that initiate and maintain a subcritical state in a thin-skinned compressive wedge. Orogen-scale analyses of Taiwan have succeeded in describing the processes and interactions that affect overall development of the thrust belt; however, relatively little is known about which processes or boundary conditions control first-order organization of strain at intermediate scales within the orogenic wedge. We investigate spatial and temporal scales of variation in the overall topographic and structural architecture of a critical wedge and explore the boundary conditions that affect very rapid shortening and erosion at intermediate scales on the order of 10^1 kilometers and 10^4–10^5 years. Causal links between the structural and synorogenic stratigraphic architecture of the foreland basin and coincidence of the Puli Topographic Embayment provide a valuable case study of the effects of changing boundary conditions (e.g., variable erodibility or strength of rocks along strike) controlling the evolution of critically tapered thin-skinned orogens. Deeper incision of river networks into a thicker sequence of unconsolidated synorogenic sediments in the central western foreland may affect the onset of a topographically subcritical state.

Citation: Wilcox, T., K. Mueller, P. Upton, Y. G. Chen, S. T. Huang, B. J. Yanites, and G. Tucker (2011), Linking Taiwan's subcritical Hsuehshan Range topography and foreland basin architecture, *Tectonics*, *30*, TC4011, doi:10.1029/2010TC002825.

1. Introduction

[2] Taiwan has been described as an ideal natural laboratory for tectonics studies where its limited size, consistent subtropical climate, well defined stratigraphy and densely instrumented thrust belt provide high-precision observations of critical wedge mechanics and kinematics [*Suppe*, 1980; *Liu et al.*, 2001; *Carena et al.*, 2002; *Fuller et al.*, 2006]. Rapid and voluminous material flux results from ~82 mm/yr of oblique plate convergence [*Yu et al.*, 1997; *Chang et al.*, 2003] and high annual precipitation occurs as a result of multiple typhoon landfalls on an annual basis [*Galewsky et al.*, 2006]. In addition to typhoons, strong ground motions produced by large earthquakes trigger many large landslides that facilitate massive and rapid sediment transport by river networks incising the island [*Galewsky et al.*, 2006; *Lin et al.*, 2006; *Yanites et al.*, 2010]. Rapid removal of material in central western Taiwan also results from the easily eroded nature of strata deformed in the thrust belt. These range from poorly indurated Quaternary sediments in the foreland and western foothills to Tertiary clastic sediments and their weakly metamorphosed equivalents in the Hsuehshan range [*Chen et al.*, 2001]. In short, Taiwan is one of the most rapidly deforming and eroding places on Earth (Figure 1). Strain in thrust belts is coupled with the rate and magnitude of erosion occurring at their subaerial surface. In turn, erosion is strongly dependent on spatial and temporal variation in local and regional climate and rock strength [*Dadson et al.*, 2003; *Dahlen and Suppe*, 1988; *England and Molnar*, 1990; *Hilley and Strecker*, 2004; *Koons et al.*, 2003; *Roe et al.*, 2006; *Willett*, 1999].

[3] Orogen-scale analyses of Taiwan have succeeded in describing the processes and interactions that affect overall development of the thrust belt, but few studies have directly assessed how variations in erosion or rheology may affect the organization of strain at intermediate scales within the orogenic wedge [*Upton et al.*, 2009a]. We use this opportunity to investigate variation in the overall topographic form of a critical wedge and explore the boundary conditions that affect strain and erosion at intermediate scales on the order of 10^1 kilometers and 10^4–10^5 years. These reflect the scale of observed changes in topography and the ages of young sediments deposited in wedge-top basins within the orogen. While numerous recent studies have defined the

[1]Department of Geological Sciences, University of Colorado at Boulder, Boulder, Colorado, USA.
[2]GNS Science, Dunedin, New Zealand.
[3]Department of Geosciences, National Taiwan University, Taipei, Taiwan.
[4]CPC Corporation, Taiwan, Miaoli, Taiwan.
[5]Department of Geological Sciences, University of Michigan, Ann Arbor, Michigan, USA.

0278-7407/11/2010TC002825

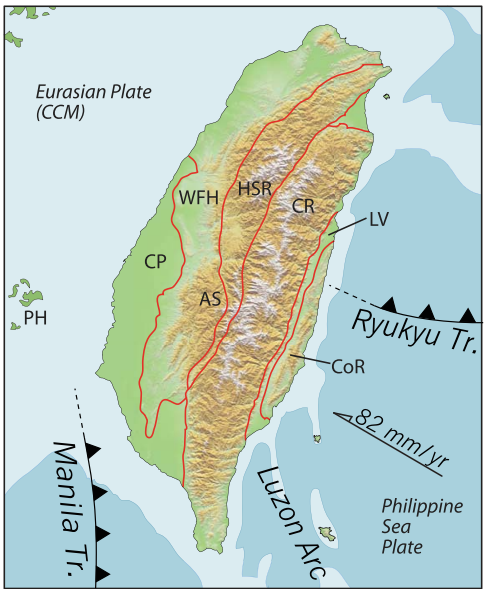

Figure 1. Tectonic setting and hillshade topography of Taiwan. Tectonic terranes of Taiwan include the Coastal Plain (CP), western foothills (WFH), Hsuehshan range (HSR), Central range (CR), Longitudinal valley (LV), and Coastal range (CoR). Also shown is Alishan (AS).

effects of variable erosion across thrust belts [*Berger et al.*, 2008; *Meigs et al.*, 2008; *Thiede et al.*, 2004; *Wobus et al.*, 2003], less is known about how thrust belts respond along their length to focused erosion [*Upton et al.*, 2009a]. We purposely confined our study to the central western region of the Island where the thrust belt absorbs purely NW-SE directed convergence within an established arc/continent collision.

1.1. Puli Topographic Embayment

[4] A striking variation in the otherwise consistently tapered shape of the western Taiwanese thrust belt is a region of relatively lower elevation we refer to as the Puli Topographic Embayment (PTE) (Figures 2 and 3). The PTE encompasses a chain of small wedge-top basins infilled with young fluviolacustrine sediments, including Puli, Yuchi, Sun-Moon Lake and Toushe (Figure 4). Previously recognized as an anomalous portion of the thrust belt [*Deffontaines et al.*, 1994; *Lu and Malavieille*, 1994; *Mueller et al.*, 2001; *Lin and Watts*, 2002; *Powell*, 2003; *Yanites et al.*, 2010], the PTE covers about a quarter of the western thrust belt. It is characterized by lower average elevation and relief relative to adjacent regions to the north and south [*Mueller et al.*, 2002; *Powell et al.*, 2002; *Wilcox et al.*, 2007]. Importantly, active compressive deformation within the topographically lower region ~50 km inboard from the leading edge of the thrust belt suggests shortening currently occurs across the entire extent of the PTE, further inboard from the active thrust front than in other adjacent regions of the thrust belt [*Mueller et al.*, 2006; *Powell*, 2003].

[5] Given the presence of deformed late Pleistocene fluviolacustrine sediments above active thrust sheets in the PTE, and their spatial correlation with a very thick sequence of readily eroded synorogenic sediments in the foreland, we hypothesize the embayment originated as a structurally dammed piggyback basin above eroded thrust sheets. This model differs from previous studies of the PTE that argue it formed as a pull-apart basin [*Lu and Malavieille*, 1994; *Lu et al.*, 2002] or as the result of indentation by the Peikang basement high [*Mouthereau et al.*, 1999; *Simoes and Avouac*, 2006] (Figure 1). The argument that the Puli and other adjacent basins formed as a result of normal faulting is based on the distribution and orientations of strike slip shear

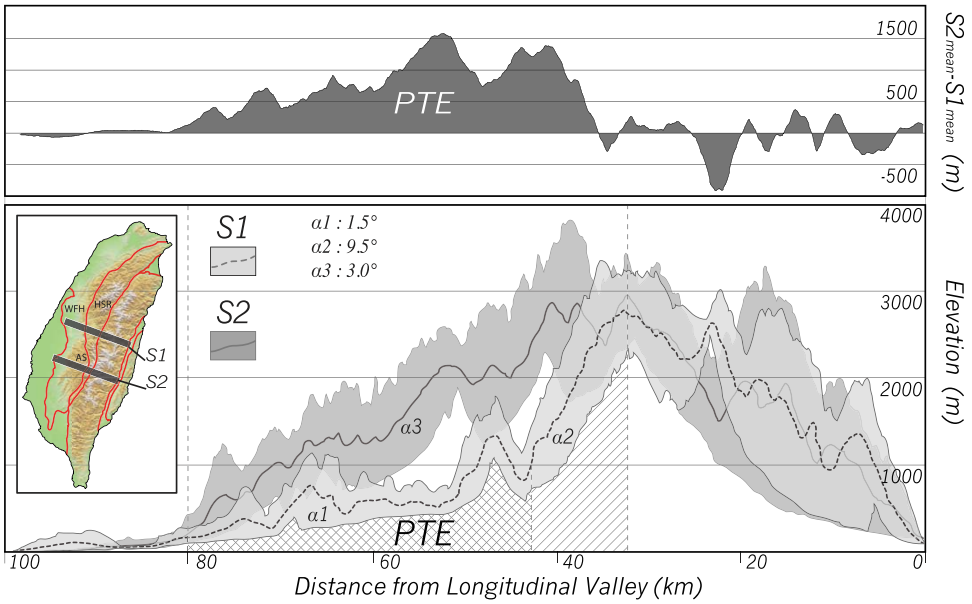

Figure 2. Swath topography of transects S1 and S2, vertically exaggerated for clarity. Minimum, maximum, and mean elevations are for 10 × 100 km areas shown in inset. Linear best fit slopes of mean topography are shown by $\alpha 1$, $\alpha 2$, and $\alpha 3$. Cross hatching is region of anomalously low surface slope, and diagonal ruling is region of anomalously high surface slope. PTE, Puli Topographic Embayment.

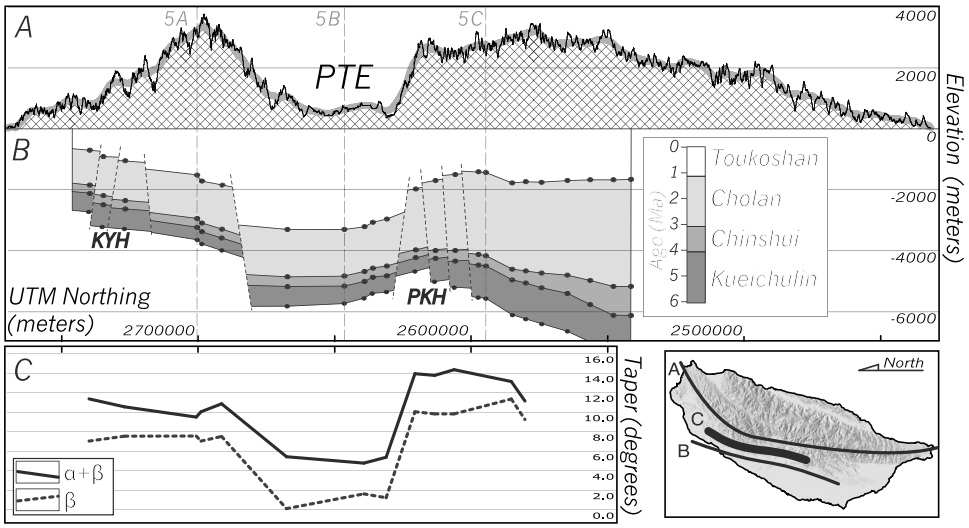

Figure 3. (a) Topographic profile and (b) foreland stratigraphic profile, both vertically exaggerated for clarity. Black topography is from 40 m DEM, and hatched gray area is moving 5 km window smoothed topography. (c) Taper is based on measurements 20–30 km inboard of the thin-skinned thrust front. Locations shown in inset. Here 5a, 5b, and 5c denote locations of cross sections in Figure 5. Depths at contacts are constrained by balanced cross sections; locations are noted with dots. PKH and KYH denote locations of Peikang and Kuanyin basement highs, shown in Figure 4.

zones within the Hsuehshan range identified by *Lu and Malavieille* [1994] and *Mouthereau et al.* [1999]. Additionally, the formation of pull-apart basins is kinematically consistent with their arguments for shear deformation. Geologic maps of Puli and the surrounding region published by Taiwan's Central Geological Survey do not show normal faults bounding any of the piggyback basins there. Numerous folds consistent with the overall contraction of the orogen are present throughout the PTE and Hsuehshan range and recent shallow seismic reflection studies within Puli show the floor of the basin is similarly folded. Alternatively, the hypothesis that the PTE results from indentation of the wedge by a structural high in the foreland basin is based on the modern position of the Peikang high and inference of its relative position to the PTE in the past [*Simoes and Avouac*, 2006], as well as the strength of the foreland and mapping of the spatial extent of the Peikang high [*Mouthereau et al.*, 2002; *Mouthereau and Petit*, 2003]. This hypothesis depends on assumptions of the shape and extent of the foreland that has already been accreted into the belt (which cannot be easily reconstructed) as well as interpretations of the shape of the Peikang high, which vary throughout the literature and do not appear to be clearly defined by any specific single physical characteristic such as depth to cover/basement contact.

[6] A detailed discussion of the depositional and erosional history within the PTE is beyond the scope of this paper, however the embayment is characterized by the following.

[7] 1. The PTE is a region of low elevation and low relief, compared to regions adjacent to the north and south, lying well within the established thrust belt.

[8] 2. Thrust sheets at the leading edge of the proto-PTE would have been covered by a thicker section of synorogenic strata, up to twice the thickness present to the north and south. These strata are still present in frontal thrust sheets.

[9] 3. Active shortening at shallow levels within the wedge (0–5 km) at the latitude of the PTE occurs further inboard from the leading edge of the belt than along the Alishan range to the south [*Mouthereau and Petit*, 2003].

[10] 4. River networks transporting sediment out of the PTE cross multiple fault-related folds, suggesting deposition of latest Pleistocene sediments within the PTE may be related to an increase in slip rate on one or more of those faults (out of sequence).

1.2. Critical Wedges

[11] Critical coulomb wedge theory is successful in describing the overall shape of submarine accretionary prisms and subaerial eroding thrust wedges like Taiwan [*Davis et al.*, 1983]. The shape of any critical coulomb wedge is controlled by the physical conditions that exist during the formation of the orogen, including the strength of the material in the wedge and pore fluid pressures throughout the wedge and at its basal decollement [*Davis et al.*, 1983]. Surface erosion has a very strong control over the internal organization of strain in critical wedges, by focusing strain into areas that exhibit a "subcritical" taper, e.g., where the balanced internal mechanics of the wedge have been upset due to a lowering of the land surface through erosion [*Konstantinovskaia and Malavieille*, 2005; *Berger et al.*, 2008; *Meigs et al.*, 2008; *Mosar*, 1999].

[12] We argue such a marked variation in the topographic form of the orogen, and therefore its subaerial taper, indicates a change in one or more of the boundary conditions that control rock uplift and erosion in the region. In this study, we address the following questions.

[13] 1. What conditions initiate the formation of and allow for the persistence of a subcritical state in an otherwise critically tapered wedge?

[14] 2. At what spatial and temporal scales can the response of the strain field to a change in boundary condi-

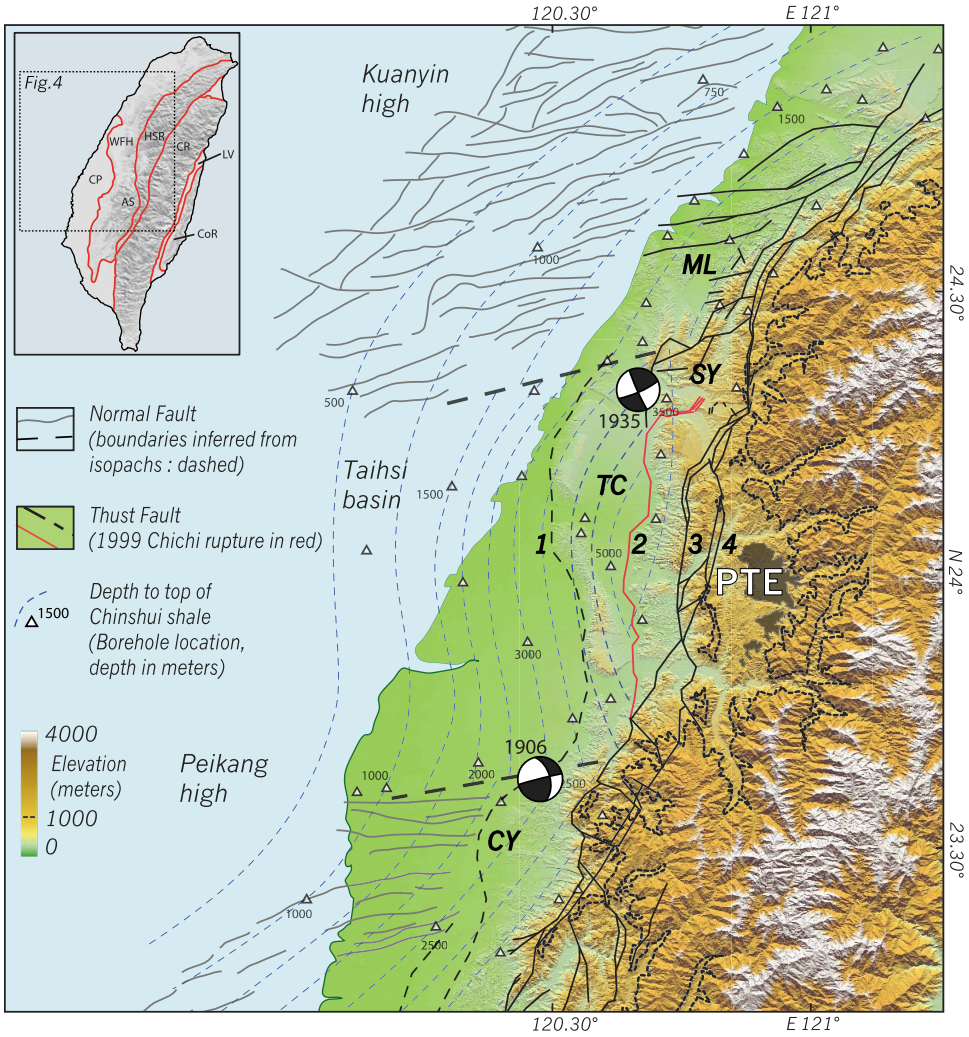

Figure 4. Map of the structural and stratigraphic architecture of the central western Taiwan foreland and western foothills. Important faults discussed in the text from west to east along 24°N latitude are the Changhua (1), Chelungpu (2), Shuangtung (3), and Shuilikeng (4). Locations: Puli Topographic Embayment (PTE, area east of Shuangtung fault, below 1000 m), Miaoli (ML), Taichung (TC), Chiayi (CY), and Sanyi overthrust (SY). Dotted black line on topography corresponds with 1000 m elevation contour. Gray shaded regions within the PTE (from north to south) outline young sediments in the Puli, Yuchi, Sun-Moon, and Toushe basins. Focal mechanisms shown for 1935 and 1906 events.

tions affecting the thrust belt be recognized in the landscape?

[15] 3. How does the erodibility of newly accreted thrust sheets control wedge taper and what role does foreland basin architecture play in that process?

2. Topography and Taper of Western Taiwan

[16] In order to characterize the differences in topography between the PTE and the consistently tapered Alishan range immediately south of the PTE, we compare 10 km × 100 km swaths of topographic data for each of these two regions. Swaths are oriented parallel to shortening direction and extend from the eastern Longitudinal Valley, which marks the boundary between the wedge and its structural backstop, to the western foreland. Calculations of wedge taper (summing of the basal and subaerial slope measurements) along the central western foothills are based on a 10 km wide swath of measurements from 13 balanced serial cross sections, 20–30 km inboard of the thin-skinned deformation front. Within the PTE, taper measurements were extended to 40 km inboard of the thin-skinned deformation front.

[17] Topography throughout the PTE, compared to the Alishan range immediately to the south, is characterized by consistently lower elevation and relief (Figure 2). Extrapolation from a linear best fit of the average elevation values of the swath data, shows that the Alishan has a constant ~3° surface slope, consistent with published characteristic subaerial taper angles for Taiwan from *Davis et al.* [1983]. In comparison, the ~1.5° average slope that exists from the foreland to the interior of the Hsuehshan range across the PTE is significantly lower, leading us to wonder whether it represents a region currently at a subcritical state. Within the PTE itself, over a distance of ~15 km, the topographic slope

is inclined ~1–2 degrees to the east, which in the convention of Taiwan's wedge would be considered a negative taper (Figure 2). As a natural result of this lower surface slope within the PTE, the slope from the eastern margin of the PTE to the drainage divide at the crest of the orogen is anomalously steep, ~9.5°.

[18] Wedge taper calculated along the western foothills of Taiwan varies depending on whether one uses the deeper Main Taiwan Detachment (MTD) or the more shallow thin-skinned base of thrusting along the western foothills as the basal surface of the critical wedge. Given the existing constraints on the deeper MTD and apparently consistent dip and depth along strike of the distribution of seismicity [*Carena et al.*, 2010], we use the better constrained shallower base of thin-skinned thrusting measured from balanced cross sections throughout the foreland and western foothills. Calculated tapers for the Miaoli and Chiayi regions are similar, with average values of ~10–11 degrees for Miaoli and ~13 degrees for Chiayi. In contrast, the PTE exhibits average values of ~5 degrees, less than half the taper of adjacent regions (Figure 3c). The changes in taper along the western thrust belt, from the Hsuehshan range, across the PTE and into the Alishan range are spatially consistent with other structural, stratigraphic and physiographic boundaries identified in this study. The difference in taper at this distance inboard from the thrust front (20–30 km) is primarily related to the relatively flat dip of the decollement below the PTE, as first presented by *Yue et al.* [2005]. The dip of the decollement below Miaoli and Chiayi are approximately −7 and −10 degrees, respectively, compared to approximately −1 below the PTE. Within the PTE, where the greater extent of cross sections allow us to calculate taper further inboard than to the north or south, we see a surprising result where due to the easterly average aspect of surface slope and the continued low dip of the basal surface of the shallow wedge, the taper we calculate is actually negative (~−2 to −3 degrees), from 30 to 40 km inboard of the thrust front. This is an unexpected and unusual observation within a critically tapered wedge, allowing us to classify this region as subcritical, especially considering that the shallow wedge deforms above recorded overpressured horizons, in purely hydrostatically pressured rocks [*Yue*, 2007].

[19] Variation of the depth and geometry of the Main Taiwan Detachment was also considered as an explanation for the change in taper, but the relatively few available constraints on this deeper decollement level suggest that it exhibits a fairly consistent depth and dip along strike below the western foothills, varying on the order of 1 km or less over distances of ~50 km or more [*Mouthereau and Petit*, 2003; *Carena et al.*, 2010]. The use of relocated seismicity to accurately define the Main Taiwan Detachment has been questioned by several authors [*Simoes et al.*, 2007; *Mouthereau et al.*, 2009] and so we calculated our determinations of wedge taper from balanced cross sections of the overriding thin-skinned wedge.

3. Foreland and Western Thrust Belt Architecture: Stratigraphy and Structure

[20] We consider the structural architecture and thicknesses of synorogenic sediments throughout the central western foreland and western foothills based on borehole measurements, seismic reflection data, published geologic maps and 23 balanced cross sections located throughout the foreland and western foothills, made available to us by the Chinese Petroleum Corporation (CPC). Seven of these cross sections have previously been published by *Yang et al.* [2007]. This paper reproduces only three representative cross sections for the north, central and south regions of our study area, in accordance with permission given by the CPC. Additionally, we support our work with findings from previously published works.

[21] The Chinese Continental Margin (CCM) supports the western foreland of Taiwan, and has been well described in terms of its depositional history and flexural response to orogenic loading [*Lin and Watts*, 2002; *Mouthereau and Petit*, 2003]. Synorogenic strata deposited in the western foreland over the last six million years record the initial migration of the foreland flexural bulge (evidenced by the flexural unconformity at the base of the Kueichulin Formation: ~6 ma) and subsequent approach and rapid erosion of the orogen (Chinshui Formation: ~4 ma; Cholan Formation: 3.1–1.1 ma; Toukoshan Formation: 1.1–0 ma) as the thrust belt advances into the foreland basin [*Chen et al.*, 2001; *Lin et al.*, 2003].

[22] The central western thrust belt of Taiwan deforms a sequence of Tertiary to Quaternary strata, divided for our purposes into preorogenic and synorogenic groups, separated by the flexural unconformity at the base of the Kueichulin Formation. Miocene and older preorogenic stratigraphic units have undergone an earlier history of extension along the CCM [*Mouthereau and Lacombe*, 2006; *Mouthereau et al.*, 2002; *Lin et al.*, 2003]. The architecture of the passive margin includes a pair of salient basement highs, buried by variable thicknesses of preorogenic and synorogenic sediments [*Byrne and Liu*, 2002; *Mouthereau et al.*, 2002]. Miocene extension of the passive margin is marked by northeast-southwest trending normal fault arrays that bound these two structural highs, now located offshore in the foreland basin west of the Taiwan thrust belt [*Mouthereau et al.*, 2002; *Lacombe et al.*, 2003]. The Kuanyin and Peikang basement highs are located northwest of the Taichung basin and west of Chiayi, respectively, buttressing the precollisional Taihsi basin (Figure 4).

3.1. Miocene-Pliocene Synorogenic Stratigraphy

[23] While the eastern portion of the early Taihsi extensional basin has been removed by erosion after its accretion into the advancing thrust belt, the western part of the basin is well defined in the modern foreland of western Taiwan. Previous work mapping isopachs and structural styles throughout the foreland delineate three distinct regions of within our study area that lie adjacent to, and correspond with, distinct topographic regions in the thrust belt, including the northern Hsuehshan, PTE and northern Alishan regions [*Mouthereau et al.*, 2002]. Measured along-strike differences in the thickness of the Kueichulin formation are relatively small and on the order of hundreds of meters, and we interpret thickness changes within these sediments as growth strata related to slip on foreland normal faults (Figure 3). Kueichulin growth strata bounded by extensional faults in the foreland are overlain by a thin sequence of early Pliocene shale of the Chinshui Formation, which does not vary in

thickness appreciably from north to south along the CCM. These strata indicate that extension of the continental shelf had ceased by the early Pliocene, marking the transition in the foreland from an extensional to a compressive setting. The physical characteristics of the Chinshui Shale are consistent with it being deposited in the distal foreland of the approaching orogenic wedge. This shale is a primary decollement level for thin-skinned deformation in central Taiwan.

3.2. Late Pliocene–Quaternary Synorogenic Sediments

[24] Spanning from late Pliocene to Quaternary time, flexural loading in the foreland of the encroaching thrust belt is recorded by the upward coarsening sequence of the Cholan and Toukoshan formations. The 3.1–1.1 Ma Cholan formation is largely uniform in thickness from north to south along the strike of the Taiwanese foreland, except where it thickens over the shelf break south of the Peikang High (from ~2000 m to almost 3500 m over a distance of 100 km (Figure 3). The geometry of the Cholan age foreland basin is well constrained from boreholes and seismic reflection profiles and is interpreted as the distal to intermediate portion of the foreland basin during the earlier stages of the development of the Taiwanese thrust belt [*Yu and Chou*, 2001; *Lin and Watts*, 2002].

[25] The Toukoshan formation is the youngest major synorogenic deposit in central western Taiwan, apart from Quaternary terraces and fluviolacustrine sediments preserved in wedge-top basins. The Toukoshan formation includes two coarsening upward members (the Hsiangshan sandstone and Huoyenshan conglomerate) that are interpreted as signaling the approach of the leading edge of the thrust belt during the last ~1.1 Ma [*Chen et al.*, 2001]. Unlike older stratigraphic units, the thickness of Toukoshan in seismic reflection profiles and boreholes varies by up to a factor of 3 from north to south along the foreland in central Taiwan [*Mouthereau et al.*, 2002]. Previous work [*Mouthereau et al.*, 1999] and cross sections made available to us by the CPC indicate that the thickness of the Toukoshan formation increases abruptly within the 60 km wide Taichung basin located immediately west of the PTE (Figures 3 and 4). The thickness of Toukoshan formation measured on a NNE-SSW trending strike-parallel profile increases from a minimum of ~1000 m near the Kuanyin basement high to over 3500 m within 50 km in the central Taiwanese foreland. These strata thin again across the Peikang basement high before increasing in thickness over the shelf edge of the CCM to the south. Notably, these marked variations in thickness occur at the same locations as underlying arrays of older Miocene normal faults bounding basement highs (Figures 3 and 4). The abrupt change in thickness in the synorogenic Toukoshan formation here suggests that older inherited structures may affect accommodation space in the foreland, driven by compressively reactivated deformation and loading of the thrust belt.

3.3. Extensional Structures in the Foreland

[26] Previous works [*Mouthereau et al.*, 2002; *Lin et al.*, 2003; *Mouthereau and Lacombe*, 2006] identify inversion of Miocene extensional faults as younger oblique thrust and strike slip faults in both the modern foreland basin and within the thrust belt itself. While not obvious in all available seismic reflection profiles at scales of individual reflectors, measurement of thickness changes in both extensional and compressional growth strata at longer intervals support a recent history (1.1 Ma to present) of minor shortening tens of kilometers into the foreland, west of the leading edge of the thin-skinned thrust belt.

[27] Evidence for normal sense displacement on these faults is recorded by variable thicknesses within the Kueichulin and older preorogenic formations that have subsequently been incorporated and deformed in thrusts and folds within the western part of the Hsuehshan range. The origin of these faults as extensional structures is well defined by stratigraphic cutoff angles and thickness changes in adjacent fault bounded blocks between the Shuangtung and Shuilikeng thrusts. In this part of the thrust belt, block bounding normal faults that cut across thrust sheets trend similarly to faults imaged in offshore seismic reflection profiles (Figure 4). We interpret these as the continuation of fault arrays evident in the foreland, due to their modern position and kinematic compatibility with the direction of thrust shortening. Some of the fault-bounded blocks retain a continuous Miocene stratigraphic record, while others contain disconformities, interpreted as a record of early migration of the flexural forebulge as the thrust belt approached from the east [*Yu and Chou*, 2001]. These faults are typically oriented at a high angle to the strike of thrust sheets and act as tear faults during shortening [*Lin*, 2005]. Strike slip focal mechanisms determined for two historic large earthquakes, attributed to slip on the Meishan fault in 1906 and the Tuntzuchiao fault in 1935, are oriented parallel to other Miocene age normal faults mapped by the CPC [*Lin*, 2005; *Shyu et al.*, 2005]. This suggests that those faults in particular may act as the main structural boundaries between the Miaoli, Taichung and Chiayi regions.

[28] Previous work has suggested that differences in structural style along the foreland and western foothills of Taiwan can be attributed to variations in the strength of basement rocks that support the foreland basin [*Mouthereau and Petit*, 2003]. Miocene age normal faults in the Miaoli and Chiayi regions also affect subsequent thin-skinned compressive strain north and south of the PTE [*Suppe*, 1986; *Mouthereau et al.*, 2002]. In particular, the northern end of the Chelungpu fault and Sanyi overthrust presents a well studied example of the interactions between advancing thin-skinned deformation that overlies preexisting structures in the foreland basement [*Yue et al.*, 2005; *Yue*, 2007].

[29] In contrast to normal faults adjacent to the Miaoli and Chiayi regions, normal faults in the Taichung region are scarce and generally not favorably oriented for reactivation as oblique or strike-slip faults. The relatively few faults that are present instead act to localize structural ramps where decollement horizons are offset by these faults [*Mouthereau et al.*, 1999; *Lee and Chan*, 2007].

4. Thrust Belt Development and Foreland Properties

[30] Discrete arrays of Miocene age normal faults partition the foreland of central Taiwan into three regions that have experienced radically different subsidence histories since 1.1 Ma, as evidenced by the thickness of Quaternary sediments in each region (Figures 3, 4, and 5). From north to south these regions are (1) the Kuanyin High, which

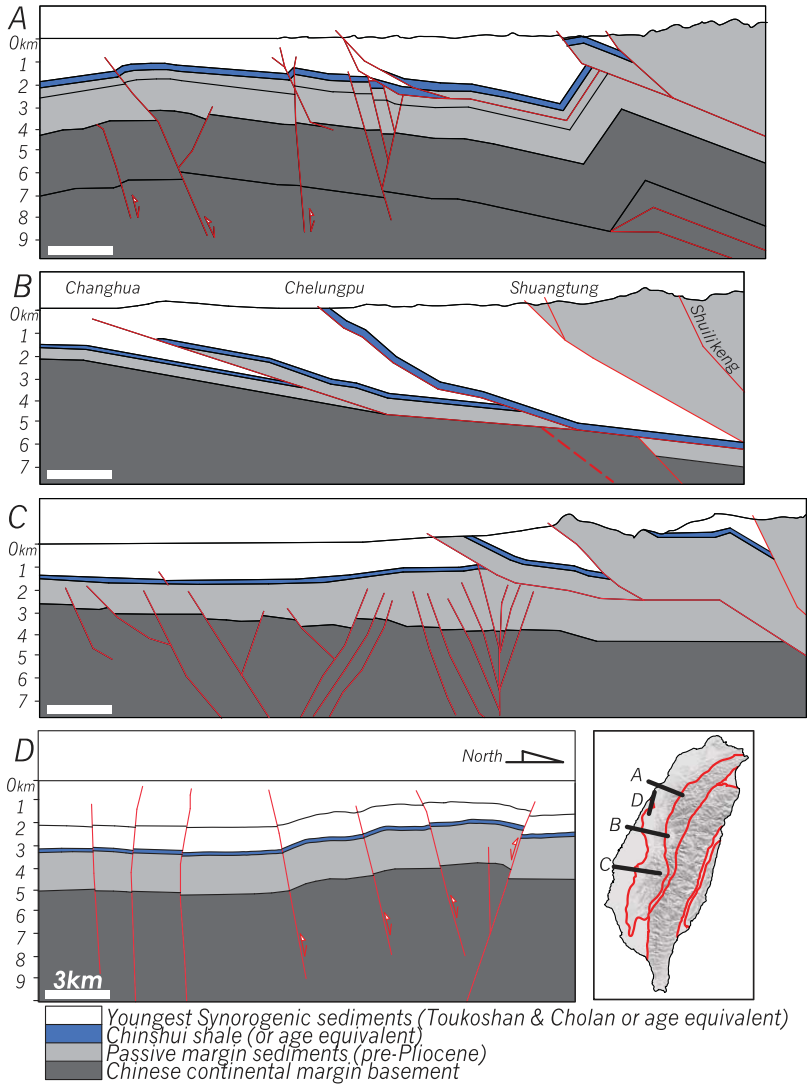

Figure 5. (a–d) Simplified balanced cross sections of the proximal foreland and western foothills, based on cross sections from the CPC. Dashed red line in Figure 5b is the approximate location of the incipient thrust ramp as determined by locations from *Chou et al.* [2009]. White scale bars represent 3 km, with no vertical exaggeration. Faults are shown in red.

includes an area of closely spaced ENE trending normal faults overlain by a relatively thinner sequence of synorogenic sediments located outboard of Miaoli; (2) a largely undeformed region adjacent to the Puli Topographic Embayment (including the Taichung basin), filled with a much thicker sequence of synorogenic strata; and (3) the Peikang High, a mildly extended region located outboard of Chiayi. Quaternary sediments in the Taiwanese foreland basin are deposited within the accommodation space resulting from flexural subsidence driven by orogenic loading [*Lin and Watts*, 2002]. Foreland basin strength is affected by existing structures, in particular older extensional fault networks reactivated by shortening and/or loading tens of kilometers in front of the leading edge of the thrust belt [*Mouthereau and Petit*, 2003]. We propose the NE-SW trending Meishan and Tuntzuchiao faults in the western foothills, which coincide with the north and south topographic boundaries of the PTE, may act as persistent structural boundaries separating discrete foreland regions that experience very different histories of proximal foreland subsidence during late Pleistocene time. The Meishan and Tuntzuchiao faults have been identified as likely sources of two large historic strike-slip earthquakes (>Mw 6) in 1906 and 1935, respectively [*Lin*, 2005; *Shyu et al.*, 2005], and may have had an effect on overall wedge development over timescales of ~10^6 years, based on the age of onset of differential subsidence across these faults. This structurally coincident difference in subsidence rates implies that the distribution of accommodation space may be variably affected through time by progressive compressional (reverse sense) reactivation of normal fault arrays with increasing proximity to the deformation front of the orogen, ultimately driving greater subsidence in the stronger central portion of the foreland (Figure 5).

[31] The thicker sequence of Toukoshan Formation in Taiwan's central foreland, and within the Taichung basin,

lies immediately west of the PTE. The margins of the area of increased fill, where Toukoshan thickens from ~1500 m to over 3300 m in as little as 20 km, are coincident with the northern and southern boundaries of the PTE, as defined by the 2000 m elevation contour of the orogen (Figure 3) [*Wilcox et al.*, 2007]. This close spatial correlation of structural boundaries with changes in topography, taper and late Pleistocene stratigraphic thickness suggests that the rheology and/or erodibility of synorogenic strata accreted into the adjacent thrust belt may exert a primary control affecting wedge development [*Upton et al.*, 2009b].

[32] While the effects of uneven erosion on wedge development in Taiwan has been explored by *Upton et al.* [2009b], our work is aimed at understanding how and why a subcritical state (as defined above) was initiated and is currently preserved in the PTE. We argue that the thick section of synorogenic sediments outboard of the PTE that capped thrust sheets accreted into the belt were more deeply incised to the level of older preorogenic strata below. This thicker central sequence sets an initial rheological template that controls thin-skinned wedge development over timescales of at least 10^4–10^5 years. A corollary follows that the sequence of thicker young synorogenic strata is weaker and more susceptible to erosion than older rocks, which is explored in section 5 on numerical modeling.

5. Modeling Critical Wedges With Variable Material Properties

[33] The recognition of along-strike variations in the material properties of the foreland and associated impacts on long-term development of wedge topography, taper and strain organization highlight the need to better understand how critical wedges respond along their length to differences in material properties (rheology) and rates of surficial processes (erosion). This section explores mechanical conditions that collectively contribute to a subcritical region within a thin-skinned orogenic wedge, which we compare to the PTE in Taiwan. Although foreland basement strength is affected by the presence of Miocene normal fault arrays [*Mouthereau and Petit*, 2003] our exploration of wedge behavior focuses solely on the internal kinematics of a thin-skinned thrust belt, rather than any processes occurring below the thin-skinned decollement.

5.1. Modeling Methods

[34] For this study, we build on previously published models of a generic fold and thrust belt of similar dimensions to Taiwan [*Upton et al.*, 2009b]. Our geometry consists of an elastic slab, representing the basement of the western foreland, beneath an elastoplastic Mohr-Coulomb wedge, representing passive margin sediments deformed in western Taiwan (Figure 6a). These are separated by an interface along which frictional slip can occur but across which no material exchange occurs. The three-dimensional numerical region extends 220 km parallel to convergence (= x) by 250 km perpendicular to convergence (= y) by 18 km vertically (= z). The eastern edge of the model consists of an elastic block simulating a rigid indentor, such as a colliding volcanic arc, that does not deform internally to a significant extent.

[35] Models were developed using the numerical code FLAC^{3D} version 3.1 (Itasca, 2006), which we have modified to accommodate local erosion. FLAC3D utilizes a modified Lagrangian finite difference technique and its use for solving geological problems is well established. The methods used have been described previously [see *Upton et al.*, 2003; *Johnson et al.*, 2004; *Upton et al.*, 2009a, 2009b].

5.2. Model Runs

[36] We present four models: model 0, a reference model, with no variation along strike, identical to model 0 of *Upton et al.* [2009b] (Figure 6b); model 1, a model with a region of lower density, weaker material in the outboard wedge, similar to model 2 of *Upton et al.* [2009b]; model 2, a model with a region of enhanced erosion within the front of the wedge (3 mm/yr compared to a background of 1 mm/yr); and model 3, a model which combines the conditions of 1 and 2 above.

[37] All models use the same velocity boundary condition: the elastic indentor acting as the backstop of the wedge moves over the decollement interface at 20 mm/yr (Figure 6a). Throughout the discussion of the models, the spatial frame of reference is analogous to that of the western Taiwanese thrust belt; the wedge verges west and "inboard" refers to positions toward the backstop to the east, while "outboard" refers to positions toward the foreland to the west. The models were run to approximately 9% strain, which is the limit of the model grid before numerical instabilities begin [*Upton et al.*, 2009b]. Erosion is imposed on the top surface of the model as a boundary condition, whereby material is removed from the model by lowering of the top surface. An erosion rate of 1 mm/yr is imposed on the western part of the model orogen while 1.3 mm/yr is imposed on the eastern part, simulating a mild orographic effect from the central uplift zone in the model. The juxtaposition of focused rapid erosion against a low background erosion rate is meant to represent the condition of a thicker section of easily erodible cover material next to harder older rocks, which have already been exposed. Given the low shortening rates (relative to Taiwan), limited strain and imposed boundary conditions of erosion, the values we determine from our models are best considered qualitatively in terms of effects on kinematic behavior observed within the model wedge. We note that increasing shortening rate to a value similar to what is observed in Taiwan would merely decrease the model run times, since the models are limited by the total strain they can accommodate.

5.3. Model Results

5.3.1. Model 1

[38] As shown previously, material variations within the wedge affect the form of the wedge [*Upton et al.*, 2009b]. Rock uplift and strain are focused into weaker material, which creates a narrow ridge at the inboard edge of the weaker material, and subsequently decreasing the magnitudes of rock uplift and strain within the adjacent region of stronger material to the east (Figure 6c). When compared to the reference model, there is a decrease in elevation inboard of the region of weaker material, creating a topographic embayment that is deeper than the embayment resulting from erosion alone (model 2). The along-strike extent of the

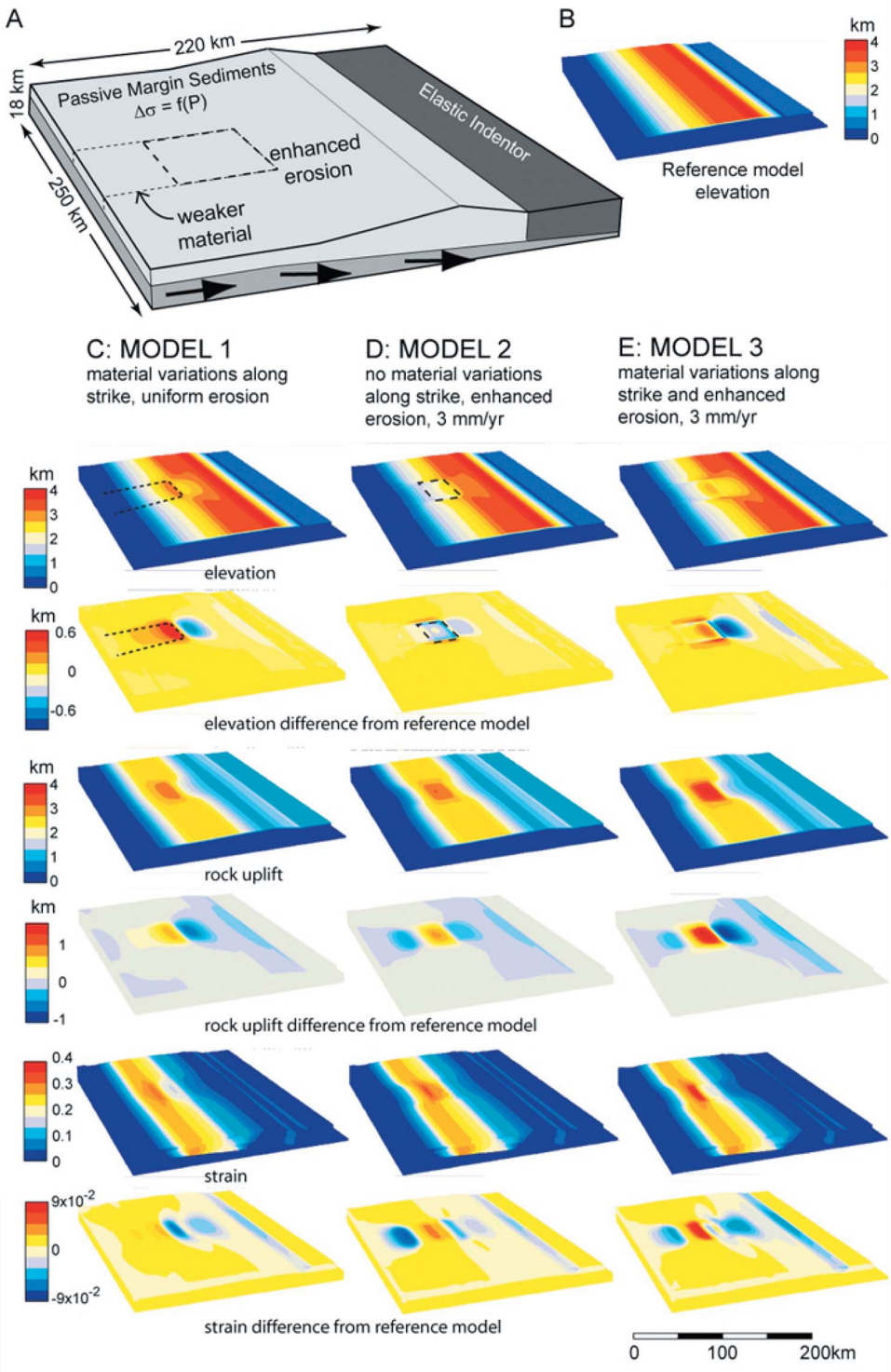

Figure 6. (a) FLAC3D model setup, (b) reference wedge, and (c, d, e) model results. Differences are achieved by subtracting a given model result from the reference model.

resulting embayment is roughly equivalent to the width of the region of weaker material ahead of it.

5.3.2. Model 2

[39] Variation of the erosion rate within the front of the wedge has a broad effect on wedge kinematics, well outside the extent of focused erosion. In fact, the impact of a focused increase in erosion rate on wedge kinematics can extend across the entire width of the wedge (Figure 6d). We note measurable differences from the reference model in elevation and magnitude of both rock uplift and strain that extend from the foreland across the wedge to the backstop. This is a result of removing mass from the orogen that

would otherwise (e.g., in the reference model) contribute to the internal stability of the critical wedge. By removing this mass the internal balance of the critical wedge is disturbed and rock uplift is focused into the region of higher erosion rate. As a result, rock uplift and strain are reduced both inboard and outboard of the rapidly eroding region, in effect balancing the overall strain budget of the wedge. As with the previous model, a decrease in rock uplift and strain inboard of the region of higher erosion creates a topographic embayment roughly equivalent in scale to the along-strike extent of the increase in erosion rate.

5.3.3. Model 3

[40] This model combines variation in material properties and focused erosion from models 1 and 2. This combination most closely represents the conditions of western Taiwan, where thick synorogenic sediments are rapidly incised above frontal thrust ramps. Because the effects on topography, rock uplift and strain are largely similar for both the individual preceding models, we see the combination of those effects is mostly constructive in this model (Figure 6e). The relief of the resulting topographic embayment is greater than in model 1 or 2, and is predicted to be at least 1000 m. The along-strike scale of the embayment is again roughly equal to the size of the regions of weak material and high erosion rate. Clear differences relative to the reference model in topography, rock uplift and strain are observed across the entire width of the wedge, similar to model 2.

6. Discussion

[41] Subcritical portions of rapidly eroding thrust wedges have been identified in a number of compressive orogens around the world. Most notably these include glaciated regions undergoing rapid and spatially limited erosion, such as within the St Elias orogen in Alaska [*Berger et al.*, 2008; *Meigs et al.*, 2008]. Additionally, sharp orographic precipitation gradients driven by the Indian Ocean monsoon have been cited as driving accelerated erosion inboard of the leading edge of the Himalayas [*Thiede et al.*, 2004; *Wobus et al.*, 2003]. In contrast, extraordinarily high rates of fluvial erosion have been associated with the development of a crustal aneurysm in the Eastern Syntaxis of the Himalaya [*Zeitler et al.*, 2001] on a scale comparable to the dimensions of the PTE. High rates of exhumation occur some 100 km from the active thrust front in the Himalaya [*Thiede et al.*, 2004; *Wobus et al.*, 2003], and at about 50–70 km in the St Elias Orogen [*Berger et al.*, 2008; *Meigs et al.*, 2008]. We note that the location of these increases in rock uplift rate and erosion rate are set by the atmospheric conditions of the orogens in which they occur; that is, they are controlled by climate, as opposed to stratigraphic architecture which acts as the primary control on variations in erosion rate in western Taiwan. The results of our models suggest that focused erosion may exert a stronger and broader influence on the organization of strain across the entire width of an active orogenic wedge than a change in material properties at the leading edge of the orogen. Even without considering changes in decollement geometry or variations in the strength of the foreland basement, we see that the combination of rapid erosion and a thick section of relatively weak material near the front of the wedge predicts a significant topographic embayment inboard of the change in boundary conditions, on the order of the scale of the PTE.

[42] The subcritical portion of the Taiwanese thrust belt formed at spatial scales of tens of kilometers, and this scale is likely controlled by the spacing of individual thrusts within the orogen [*Upton et al.*, 2009b] and by the spacing of preexisting normal fault arrays in the foreland. This scaling is analogous to the observations of relative scale in our models, where the spatial scale of variations in foreland conditions controls the along-strike extent of variations in topography and strain within the wedge.

[43] Precipitation in Taiwan is characterized by very large rainfall events associated with large typhoons, which are capable of delivering more than a meter of rainfall over a period of 24 h [*Galewsky et al.*, 2006]. While precipitation increases with elevation in western Taiwan, rainfall along the Foothills Belt and Hsuehshan range is essentially similar along the length of the thrust belt and is in fact contemporarily lower in the PTE itself [*Galewsky et al.*, 2006]. Contemporary erosion rates within the PTE are actually quite low, whereas the incision of stream channel networks (and related removal of mass) is focused outboard of the PTE within the active foothills of the orogen [*Dadson et al.*, 2003]. These sediments are transported to the foreland where variably thick (~2–5 km) sections of synorogenic strata have yet to be accreted at the front of the orogen.

[44] We posit that rapid incision into exposed sections of Toukoshan and Cholan formations in active thrust sheets is likely related to their unconsolidated nature and negligible diagenetic history during burial within the foreland basin [*Chen et al.*, 2001]. The primary control on incision of river networks and focusing of erosion into the proto-PTE is likely related to the variable thickness of synorogenic strata that cap active thrust sheets in the foreland. Removing the relatively thinner sequences of Pleistocene sediments that capped thrust sheets north and south of the proto-PTE results in relatively earlier exposure of the harder and less erodible Miocene and Oligocene rocks in the northern Hsuehshan and northern Alishan ranges. River networks would thus naturally focus and more deeply incise the thicker section of synorogenic sediment capping thrust sheets within the proto-PTE (Figure 7). As observed in our models, the formation of a topographic embayment is predicted inboard of a region undergoing focused rapid erosion, due to the disturbance of the internal mass balance of the critical wedge and subsequent reorganization of strain.

[45] The coincidence of mapped locations of abrupt changes in thickness of late Pleistocene synorogenic fill, lower average topography within the PTE and the locations of at least three recent (1906–1999) large earthquakes (>Mw 6) that occurred along topographic and structural boundaries of the embayment can be attributed to the variable structural architecture and contemporary kinematics of the central Taiwan foreland. This suggests that the history of subsidence in the foreland controls both denudation and reorganization of strain in the thrust belt, such that a subcritical state is initiated and maintained at timescales of up to 10^6 years. We propose that variable subsidence of the foreland basin, controlled by the orientations and spatial distributions of reactivated older structures, has a profound influence on the distribution of strain within the eroding

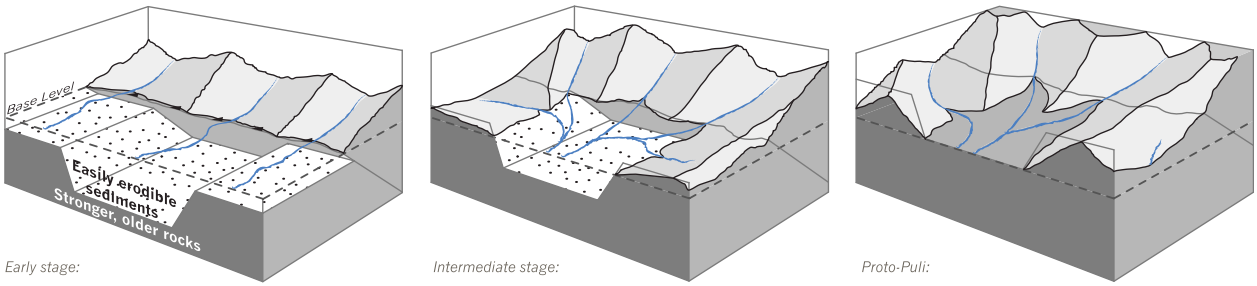

Figure 7. Schematic block diagrams of land surface evolution, controlled by distribution of thicknesses of easily eroded synorogenic sediments. Early stage: foreland template is set by varying subsidence along strike, with thicker sequence of easily erodible sediment in central region. Intermediate stage: material is accreted into wedge initiating rock uplift. As rocks are brought above local base level, different rheologies respond to river incision at different rates and drainages are reorganized. Proto-Puli: all synorogenic sediment is flushed from uplifted region into the foreland basin. Beginning at the intermediate stage, focused erosion should start to affect topographic growth and strain organization (see Figure 6 and section 6). Dashed line represents local base level, and textured blue lines represent rivers.

portion of the thrust belt. Potentially this influence could be observed across the entire width of the orogenic wedge.

7. Summary

[46] The contemporary presence of a region of anomalously low topography within the Taiwanese thrust belt provides insight into the processes that initiate and maintain a subcritical condition in a thin-skinned compressive wedge. The causal links between the foreland structural architecture, synorogenic stratigraphic architecture and presence of the Puli Topographic Embayment provides a valuable case study of the effects of changing boundary conditions controlling the evolution of critical thin-skinned orogens. Moreover, the preexisting structural architecture within the foreland appears to strongly influence subsidence behavior, resulting in abrupt and localized differences in the thickness of foreland basin fill. Deeper incision of river networks into the thicker sequence of unconsolidated fill in the central western foreland may then focus erosion within the proto-PTE, initiating the onset of a subcritical state. The onset of focused erosion related to the PTE is unknown. However, estimates based on the thickness of Toukoshan strata, restoration of slip along the Chelungpu and Shuangtung thrusts and an assumption of ~45 mm/yr of shortening across the entire foothills belt suggest the PTE may have been initiated between ~700 and 500 Ka. This suggests that a subcritical state may exist within the western Taiwanese thrust belt for a significant fraction of its total development.

[47] **Acknowledgments.** We would like to acknowledge the Chinese Petroleum Company, Wen-Rong Chi, and Kenn-Ming Yang for access to their data and many helpful discussions. John Suppe and Tony Watts were also immensely helpful in offering comments and enlightening discussion. This paper also benefited from the constructive reviews of Frederic Mouthereau and Bruce Shyu. We would additionally like to thank Ling-Ho Chung, Po-Nong Lee, and Shao-Yi Huang for logistical support in the field. This research was funded by NSF grant EAR-0510971.

References

Berger, A. L., et al. (2008), Quaternary tectonic response to intensified glacial erosion in an orogenic wedge, *Nat. Geosci.*, *1*, 793–799, doi:10.1038/ngeo334.

Byrne, T. B., and C.-S. Liu (2002), Introduction to the geology and geophysics of Taiwan, in *Geology and Geophysics of an Arc-Continent Collision, Taiwan*, edited by T. B. Byrne and C.-S. Liu, *Spec. Pap. Geol. Soc. Am.*, *358*, v–viii.

Carena, S., J. Suppe, and H. Kao (2002), Active detachment of Taiwan illuminated by small earthquakes and its control of first-order topography, *Geology*, *30*, 935–938, doi:10.1130/0091-7613(2002)030<0935:ADOTIB>2.0.CO;2.

Carena, S., J. Suppe, and Y.-M. Wu (2010), Lithospheric structure of Taiwan from seismicity and crustal tomography, *Geol. Soc. Am. Abstr. Programs*, *42*(5), 78.

Chang, C. P., T. Y. Chang, J. Angelier, H. Kao, J. C. Lee, and S. B. Yu (2003), Strain and stress field in Taiwan oblique convergent system: Constraints from GPS observation and tectonic data, *Earth Planet. Sci. Lett.*, *214*, 115–127, doi:10.1016/S0012-821X(03)00360-1.

Chen, W.-S., K. D. Ridgway, C. S. Horng, Y. G. Chen, K. S. Shea, and M. G. Yeh (2001), Stratigraphic architecture, magnetostratigraphy, and incised-valley systems of the Pliocene-Pleistocene collisional marine foreland basin of Taiwan, *Geol. Soc. Am. Bull.*, *113*, 1249–1271, doi:10.1130/0016-7606(2001)113<1249:SAMAIV>2.0.CO;2.

Chou, C., J. Suppe, S. Carena, and S. Huang (2009), Advances in 3D imaging of the geometry of the Chi-Chi earthquake thrust system in western Taiwan, *Eos Trans AGU*, *90*(52), *Fall Meet. Suppl.*, Abstract T33B-1896.

Dadson, S. J., et al. (2003), Links between erosion, runoff variability and seismicity in the Taiwan orogen, *Nature*, *426*(6967), 648–651, doi:10.1038/nature02150.

Dahlen, F. A., and J. Suppe (1988), Mechanics, growth, and erosion of mountain belts, in *Processes in Continental Lithospheric Deformation*, edited by S. P. Clark, B. C. Burchfiel, and J. Suppe, *Spec. Pap. Geol. Soc. Am.*, *218*, 161–178.

Davis, D., J. Suppe, and F. A. Dahlen (1983), Mechanics of fold-and-thrust belts and accretionary wedges, *J. Geophys. Res.*, *88*, 1153–1172, doi:10.1029/JB088iB02p01153.

Deffontaines, B., J.-C. Lee, J. Angelier, J. Carvalho, and J.-P. Rudant (1994), New geomorphic data on the active Taiwan orogen: A multisource approach, *J. Geophys. Res.*, *99*, 20,243–20,266, doi:10.1029/94JB00733.

England, P. C., and P. Molnar (1990), Surface uplift, uplift of rocks, and exhumation of rocks, *Geology*, *18*, 1173–1177, doi:10.1130/0091-7613(1990)018<1173:SUUORA>2.3.CO;2.

Fuller, C. W., S. D. Willett, D. Fisher, and C. Y. Lu (2006), A thermomechanical wedge model of Taiwan constrained by fission-track thermochronometry, *Tectonophysics*, *425*, 1–24, doi:10.1016/j.tecto.2006.05.018.

Galewsky, J., C. P. Stark, S. Dadson, C.-C. Wu, A. H. Sobel, and M.-J. Horng (2006), Tropical cyclone triggering of sediment discharge in Taiwan, *J. Geophys. Res.*, *111*, F03014, doi:10.1029/2005JF000428.

Hilley, G. E., and M. R. Strecker (2004), Steady state erosion of critical Coulomb wedges with applications to Taiwan and the Himalaya, *J. Geophys. Res.*, *109*, B01411, doi:10.1029/2002JB002284.

Johnson, S. E., R. H. Vernon, and P. Upton (2004), Foliation development and progressive strain-rate partitioning in the crystallizing carapace of

a tonalite pluton: Microstructural evidence and numerical modeling, *J. Struct. Geol.*, *26*, 1845–1865.

Konstantinovskaia, E., and J. Malavieille (2005), Erosion and exhumation in accretionary orogens: Experimental and geological approaches, *Geochem. Geophys. Geosyst.*, *6*, Q02006, doi:10.1029/2004GC000794.

Koons, P. O., R. J. Norris, D. Craw, and A. F. Cooper (2003), Influence of exhumation on the structural evolution of transpressional plate boundaries: An example from the Southern Alps, New Zealand, *Geology*, *31*, 3–6, doi:10.1130/0091-7613(2003)031<0003:IOEOTS>2.0.CO;2.

Lacombe, O., F. Mouthereau, J. Angelier, H.-T. Chu, and J.-C. Lee (2003), Frontal belt curvature and oblique ramp development at an obliquely collided irregular margin: Geometry and kinematics of the NW Taiwan fold-thrust belt, *Tectonics*, *22*(3), 1025, doi:10.1029/2002TC001436.

Lee, J.-C., and Y.-C. Chan (2007), Structure of the 1999 Chi-Chi earthquake rupture and interaction of thrust faults in the active fold belt of western Taiwan, *J. Asian Earth Sci.*, *31*, 226–239, doi:10.1016/j.jseaes.2006.07.024.

Lin, A. T., and A. B. Watts (2002), Origin of the West Taiwan basin by orogenic loading and flexure of a rifted continental margin, *J. Geophys. Res.*, *107*(B9), 2185, doi:10.1029/2001JB000669.

Lin, A. T., A. B. Watts, and S. P. Hesselbo (2003), Cenozoic stratigraphy and subsidence history of the South China Sea margin in the Taiwan region, *Basin Res.*, *15*, 453–478, doi:10.1046/j.1365-2117.2003.00215.x.

Lin, C. W., S. H. Liu, S. Y. Lee, and C. C. Liu (2006), Impacts of the Chi-Chi earthquake on subsequent rainfall-induced landslides in central Taiwan, *Eng. Geol. Amsterdam*, *86*, 87–101, doi:10.1016/j.enggeo.2006.02.010.

Lin, Y. N. (2005), Surface deformation and seismogenic structure model of the 1935 Hsinchu-Taichung earthquake (Mgr = 7.1), in Miaoli, northwestern Taiwan, M.Sc. thesis, 92 pp., Natl. Taiwan Univ., Taipei.

Liu, T. K., S. Hsieh, Y. G. Chen, and W. S. Chen (2001), Thermokinematic evolution of the Taiwan oblique-collision mountain belt as revealed by zircon fission track dating, *Earth Planet. Sci. Lett.*, *186*, 45–56, doi:10.1016/S0012-821X(01)00232-1.

Lu, C.-Y., and J. Malavieille (1994), Oblique convergence, indentation and rotation tectonics in the Taiwan Mountain Belt: Insights from experimental modeling, *Earth Planet. Sci. Lett.*, *121*, 477–494, doi:10.1016/0012-821X(94)90085-X.

Lu, C.-Y., H.-T. Chu, J.-C. Lee, Y.-C. Chan, K.-J. Chang, and F. Mouthereau (2002), The 1999 Chi-Chi Taiwan earthquake and basement impact thrust kinematics, *West. Pac. Earth Sci.*, *2*(2), 181–190.

Meigs, A., S. Johnston, J. Garver, and J. Spotila (2008), Crustal-scale structural architecture, shortening, and exhumation of an active, eroding orogenic wedge (Chugach, St Elias range, southern Alaska), *Tectonics*, *27*, TC4003, doi:10.1029/2007TC002168.

Mosar, J. (1999), Present-day and future tectonic underplating in the western Swiss Alps: Reconciliation of basement/wrench-faulting and décollement folding of the Jura and Molasse basin in the Alpine foreland, *Earth Planet. Sci. Lett.*, *173*, 143–155, doi:10.1016/S0012-821X(99)00238-1.

Mouthereau, F., and O. Lacombe (2006), Inversion of the Paleogene continental margin and thick-skinned deformation in the western foreland of Taiwan, *J. Struct. Geol.*, *28*, 1977–1993, doi:10.1016/j.jsg.2006.08.007.

Mouthereau, F., and C. Petit (2003), Rheology and strength of the Eurasian continental lithosphere in the foreland of the Taiwan collision belt: Constraints from seismicity, flexure, and structural styles, *J. Geophys. Res.*, *108*(B11), 2512, doi:10.1029/2002JB002098.

Mouthereau, F., O. Lacombe, B. Deffontaines, J. Angelier, H. T. Chu, and C. T. Lee (1999), Quaternary transfer faulting and belt front deformation at Pakuashan (western Taiwan), *Tectonics*, *18*(2), 215–230.

Mouthereau, F., B. Deffontaines, O. Lacombe, and J. Angleier (2002), Variations along the strike of the Taiwan thrust belt: Basement control of structural style, wedge geometry, and kinematics, in *Geology and Geophysics of an Arc-Continent Collision, Taiwan*, edited by T. B. Byrne and C.-S. Liu, *Spec. Pap. Geol. Soc. Am.*, *358*, 35–58.

Mouthereau, F., C. Fillon, and K.-F. Ma (2009), Distribution of strain rates in the Taiwan orogenic wedge, *Earth Planet. Sci. Lett.*, *284*, 361–385, doi:10.1016/j.epsl.2009.05.005.

Mueller, K. J., Y. Chen, and G. Kier (2001), Erosion-induced backstepping and reactivation of the Chelungpu thrust: Implications for patterns of modern strain release in west-central Taiwan, *Eos Trans. AGU*, *82*(47), Fall Meet. Suppl., Abstract T32A-0878.

Mueller, K., Y. Chen, and L. Powell (2002), Modern strain and structural architecture of the central Taiwanese orogen: Evidence for active backstepping in response to erosion?, *Eos Trans. AGU*, *83*(47), Fall Meet. Suppl., Abstract T61B-1279.

Mueller, K., T. Wilcox, and Y. Chen (2006), Subcritical thrust wedge development in west-central Taiwan in response to rapid erosion of synorogenic sediments, *Eos Trans. AGU*, *87*(52), Fall Meet. Suppl., Abstract T11A-0433.

Powell, L. K. (2003), Feedback between erosion and fault reactivation in the Puli Basin: Hsüehshan Belt of central Taiwan, M.S. thesis, 61 pp., Univ. of Colo. at Boulder, Boulder.

Powell, L., K. Mueller, and Y. Chen (2002), Geomorphic constraints on patterns of shortening and erosion in the Puli Basin: Hinterland of the central Taiwan Thrust Belt, *Eos Trans. AGU*, *83*(47), Fall Meet. Suppl., Abstract T61B-1270.

Roe, G. H., D. B. Stolar, and S. D. Willett (2006), Response of a steady-state critical wedge orogen to changes in climate and tectonic forcing, in *Tectonics, Climate, and Landscape Evolution*, *Spec. Pap. Geol. Soc. Am.*, *398*, 227–239.

Shyu, J. B. H., K. Sieh, Y.-G. Chen, and C.-S. Liu (2005), Neotectonic architecture of Taiwan and its implications for future large earthquakes, *J. Geophys. Res.*, *110*, B08402, doi:10.1029/2004JB003251.

Simoes, M., and J. P. Avouac (2006), Investigating the kinematics of mountain building in Taiwan from the spatiotemporal evolution of the foreland basin and western foothills, *J. Geophys. Res.*, *111*, B10401, doi:10.1029/2005JB004209.

Simoes, M., J. P. Avouac, Y.-G. Chen, A. K. Singhvi, C.-Y. Wang, M. Jaiswal, Y.-C. Chan, and S. Bernard (2007), Kinematic analysis of the Pakuashan fault tip fold, west central Taiwan: Shortening rate and age of folding inception, *J. Geophys. Res.*, *112*, B03S14, doi:10.1029/2005JB004198.

Suppe, J. (1980), Imbricated structure of western foothills belt, south-central Taiwan, *Pet. Geol. Taiwan*, *17*, 1–16.

Suppe, J. (1986), Reactivated normal faults in the western Taiwan fold-and-thrust belt, *Mem. Geol. Soc. China*, *7*, 187–200.

Thiede, R. C., B. Bookhagen, J. R. Arrowsmith, E. R. Sobel, and M. R. Strecker (2004), Climatic control on rapid exhumation along the southern Himalayan front, *Earth Planet. Sci. Lett.*, *222*, 791–806, doi:10.1016/j.epsl.2004.03.015.

Upton, P., P. O. Koons, and D. Eberhart-Phillips (2003), Extension and partitioning in an oblique subduction zone, New Zealand: Constraints from three-dimensional numerical modeling, *Tectonics*, *22*(6), 1068, doi:10.1029/2002TC001431.

Upton, P., P. O. Koons, D. Craw, C. M. Henderson, and R. Enlow (2009a), Along-strike differences in the Southern Alps of New Zealand: Consequences of inherited variation in rheology, *Tectonics*, *28*, TC2007, doi:10.1029/2008TC002353.

Upton, P., K. Mueller, and Y.-G. Chen (2009b), Three-dimensional numerical models with varied material properties and erosion rates: Implications for the mechanics and kinematics of compressive wedges, *J. Geophys. Res.*, *114*, B04408, doi:10.1029/2008JB005708.

Wilcox, T., K. Meuller, and Y. Chen (2007), Systematic variations in synorogenic fill architecture and fault offsets along strike across the Puli Topographic Embayment: Quaternary strain gradients in the central western foothills and Taiwanese foreland basin, *Eos Trans. AGU*, *88* (52), Fall Meet. Suppl., Abstract T32C-07.

Willett, S. D. (1999), Orogeny and orography: The effect of erosion on the structure of mountain belts, *J. Geophys. Res.*, *104*(B12), 28,957–28,981, doi:10.1029/1999JB900248.

Wobus, C. W., K. V. Hodges, and K. X. Whipple (2003), Has focused denudation sustained active thrusting at the Himalayan topographic front?, *Geology*, *31*, 861–864, doi:10.1130/G19730.1.

Yang, K.-M., S.-T. Huang, J.-C. Wu, H.-H. Ting, W.-W. Mei, M. Lee, H.-H. Hsu, and C.-J. Lee (2007), 3D geometry of the Chelungpu Thrust System in central Taiwan: Its implications for active tectonics, *Terr. Atmos. Ocean. Sci.*, *18*(2), 143–181, doi:10.3319/TAO.2007.18.2.143(TCDP).

Yanites, B. J., G. E. Tucker, K. J. Mueller, Y.-G. Chen, T. Wilcox, S.-Y. Huang, and K.-W. Shi (2010), Incision and channel morphology across active structures along the Peikang River, central Taiwan: Implications for the importance of channel width, *Geol. Soc. Am. Bull.*, *122*, 1192–1208.

Yu, H. S., and Y. W. Chou (2001), Characteristics and development of the flexural forebulge and basal unconformity of western Taiwan Foreland Basin, *Tectonophysics*, *333*, 277–291, doi:10.1016/S0040-1951(00)00279-1.

Yu, S. B., H. Y. Chen, and L. C. Kuo (1997), Velocity field of GPS stations in the Taiwan area, *Tectonophysics*, *274*, 41–59, doi:10.1016/S0040-1951(96)00297-1.

Yue, L. F. (2007), Active structural growth in central Taiwan in relationship to large earthquakes and pore-fluid pressures, Ph.D. dissertation, 272 pp., Princeton University, Princeton, N. J.

Yue, L. F., J. Suppe, and J. H. Hung (2005), Structural geology of a classic thrust belt earthquake: The 1999 Chi-Chi earthquake Taiwan (M−w = 7.6), *J. Struct. Geol.*, *27*, 2058–2083, doi:10.1016/j.jsg.2005.05.020.

Zeitler, P. K., et al. (2001), Erosion, Himalayan geodynamics and the geomorphology of metamorphism, *GSA Today*, *11*, 4–8, doi:10.1130/1052-5173(2001)011<0004:EHGATG>2.0.CO;2.

Y. G. Chen, Department of Geosciences, National Taiwan University, 1, Section 4, Roosevelt Road, Taipei, 10617, Taiwan.

S. T. Huang, CPC Corporation, Taiwan, 1 Ta Yuan, Wen Fa Road, Wen Sheng, Miaoli, 36042, Taiwan.

K. Mueller, G. Tucker, and T. Wilcox, Department of Geological Sciences, University of Colorado at Boulder, 2200 Colorado Ave., Boulder, CO 80309, USA. (tarkawilcox@gmail.com)

P. Upton, GNS Science, PO Box 3036, Lower Hut 5040, Dunedin 9054, New Zealand.

B. J. Yanites, Department of Geological Sciences, University of Michigan, 1100 N. University Ave., Ann Arbor, MI 48109, USA.